Assessment of primary energy conversions of oscillating water columns. II. Power take-off and validations

Wanan Sheng, Raymond Alcorn, and Anthony Lewis

Citation: Journal of Renewable and Sustainable Energy **6**, 053114 (2014); doi: 10.1063/1.4896851
View online: http://dx.doi.org/10.1063/1.4896851
View Table of Contents: http://scitation.aip.org/content/aip/journal/jrse/6/5?ver=pdfcov
Published by the AIP Publishing

Assessment of primary energy conversions of oscillating water columns. II. Power take-off and validations

Wanan Sheng, Raymond Alcorn, and Anthony Lewis
Beaufort Research—Hydraulics and Maritime Research Centre, University College Cork, Cork, Ireland

(Received 14 May 2014; accepted 19 September 2014; published online 29 September 2014)

This is the second part of the assessment of primary energy conversions of oscillating water columns (OWCs) wave energy converters. In the first part of the research work, the hydrodynamic performance of OWC wave energy converter has been extensively examined, targeting on a reliable numerical assessment method. In this part of the research work, the application of the air turbine power take-off (PTO) to the OWC device leads to a coupled model of the hydrodynamics and thermodynamics of the OWC wave energy converters, in a manner that under the wave excitation, the varying air volume due to the internal water surface motion creates a reciprocating chamber pressure (alternative positive and negative chamber pressure), whilst the chamber pressure, in turn, modifies the motions of the device and the internal water surface. To do this, the thermodynamics of the air chamber is first examined and applied by including the air compressibility in the oscillating water columns for different types of the air turbine PTOs. The developed thermodynamics is then coupled with the hydrodynamics of the OWC wave energy converters. This proposed assessment method is then applied to two generic OWC wave energy converters (one bottom fixed and another floating), and the numerical results are compared to the experimental results. From the comparison to the model test data, it can be seen that this numerical method is capable of assessing the primary energy conversion for the oscillating water column wave energy converters. © *2014 AIP Publishing LLC*. [http://dx.doi.org/10.1063/1.4896851]

I. INTRODUCTION

For a practical oscillating water column (OWC) wave energy plant, the volume of and the pressure in the air chamber can be large enough so that the air compressibility can be invoked, and a 'spring-like effect' can occur (Falcao *et al.*[1]). However, in a model scale, the volume of and the chamber pressure in the air chamber are both scaled down, and they both may be too small, so that the air compressibility is not correctly scaled in the model test of the OWC wave energy converters, especially when the small test models at the early development stages of the wave energy conversion are used, because as shown by Weber[2] and Sheng *et al.*,[3] the air compressibility is not fully scalable according to the conventional Froude similitude. To approximately represent the air compressibility in the model scale, the air chamber must be designed to be much larger than that from the Froude similarity, and Weber[2] suggested that the length of the air chamber must kept same regardless of the scale ratio used in the model test. Sheng *et al.*[3] pointed out that keeping the same air chamber height is one of many choices, and different approaches can be attainable if an appropriate air chamber volume is produced. Nonetheless, this has highlighted the difficulties in representing the air compressibility in the model test. Hence, a reliable numerical method capable of assessing the air compressibility in the air chamber in an OWC wave energy converter is very desirable.

Sarmento *et al.*[4] have proposed a linearized formula for the flowrate through the power take-off system, based on an assumption of an isentropic process in the air chamber, and Sheng *et al.*[5] have recently formulated full thermodynamic equations for the air flow in the chamber by incorporating the power take-off system for studying the air compressibility. The

development is based on the same principle of an isentropic process as many other researchers (Refs. 1, 4, and 6–10, see Figure 1). For validations, the developed method has been compared to the test data from a special piston test, in which the piston, representing the internal water surface motion, is connected to a test rig. The test rig could provide a much powerful drive to the piston than that from the normal tank test. Hence, it is possible to obtain air compressibility in the well-controlled laboratory conditions (Sheng *et al.*[5,11]). The validation has shown the developed numerical method is capable of predicting the compressibility.

Coupling the hydrodynamics and thermodynamics yields time-domain dynamic equations for the OWC wave energy converters. Solving the coupled time-domain equations, we could assess the performance and the power conversion of the OWC wave energy converters. To validate the developed method, detailed comparisons are made to the experimental data for the dynamic performances for the generic OWC devices.

II. THERMODYNAMICS IN THE AIR CHAMBER

For converting the pneumatic energy into useful energy in the OWC wave energy converters, air turbine power take-offs (PTOs) are frequently used. So far, two types of self-rectifying air turbines are popularly employed in practical wave energy converters, namely the Wells turbine and impulse turbine. For a given rotating speed, an air turbine PTO could be a linear PTO, for example, the Wells turbine, in which the turbine has a linear relation between the chamber pressure and the flowrate; or a nonlinear PTO, for instance, the impulse turbine, which very much performs like an orifice with an appropriate discharging coefficient. A novel bi-radial turbine has been recently developed by Falcao *et al.*,[6,12] which has shown a promising energy conversion efficiency. In this section, all three types of the air turbines will be discussed further.

Following the suggestion of Falcao *et al.*,[7] the definition of the PTO relation is to use the mass flowrate rather than the volume flowrate, so that we may avoid the problem of the flow density pass through the air turbine. Following this convention, the air turbine PTO will be mathematically expressed as the relation of the pressure drop cross the PTO (it can be also called chamber pressure, or gauge pressure), p, and the mass flowrate, $\dot{m}$, through the air turbine PTO (also see Sheng *et al.*[13]). For a completeness, the relevant formulas are simply given here, but more details can be found in Sheng *et al.*[5]

A. Mass conservation

In the air chamber, the mass of the air is calculated as

$$m = \rho V, \tag{1}$$

where V is the air volume in the air chamber, and ρ the density of the air in the chamber.

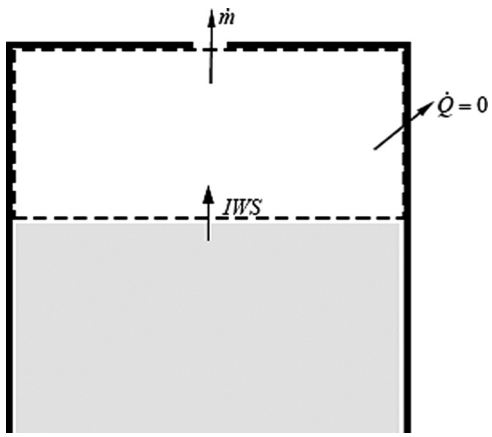

FIG. 1. A control volume for the thermodynamic system in an OWC device.

Hence, the mass flowrate through the PTO is simply the differentiation with regard to time, given by

$$\dot{m} = \dot{\rho}V + \rho\dot{V}. \tag{2}$$

The first term in RHS indicates an increase of the mass in the air chamber due to an increase of the air density if the air volume is constant, and the second term means the mass increase due to the increase of the air volume if the density is constant. However, for an open system shown in Figure 1, the mass increase or decrease happens only when the air flow passing the PTO. It must be noted that a positive mass flowrate means that air is being inhaled into the chamber, so that the air mass in the air chamber is increased, and a negative mass flowrate means some air is exhaled from the air chamber. One would also understand that in the OWC devices, the air volume change is made only because of the internal water surface motion (IWS).

B. Ideal air

To simplify the analysis of the thermodynamic problem in the OWC wave energy conversion, the air in the chamber is considered as isentropic, which gives a state equation for a partially open system of the control volume shown in Figure 1 as

$$\frac{p_c}{\rho^\gamma} = C_0, \tag{3}$$

where γ is the specific heat ratio of the air ($\gamma = 1.4$), and C_0 a constant.

Equation (3) can be further expressed as

$$\frac{p_0 + p}{\rho^\gamma} = \frac{p_0}{\rho_0^\gamma}, \tag{4}$$

where p_0 is the atmospheric pressure and ρ_0 the air density in the atmosphere.

So,

$$\rho = \rho_0\left(1 + \frac{p}{p_0}\right)^{\frac{1}{\gamma}}. \tag{5}$$

A linearised form of the Eq. (5) can be easily derived if the absolute chamber pressure p is much smaller than the atmospheric pressure, p_0 (about 10^5 Pa, and practically, it is true that the atmospheric pressure is significantly larger than the possibly largest chamber pressure occurred in a practical OWC device). Hence,

$$\rho = \rho_0\left(1 + \frac{p}{\gamma p_0}\right). \tag{6}$$

From Eq. (6), its differential form is

$$\dot{\rho} = \frac{\rho_0}{\gamma p_0}\dot{p}. \tag{7}$$

Substituting (6) and (7) into (2) yields

$$\dot{m} = \frac{\rho_0 V}{\gamma p_0}\dot{p} + \rho_0\left(1 + \frac{p}{\gamma p_0}\right)\dot{V}. \tag{8}$$

C. Linear PTO (Wells turbine)

The famous Wells turbine is normally regarded as a linear air turbine. For such a linear air turbine, the chamber pressure and the mass flowrate have a relation as

$$p = -k_1 \dot{m}, \tag{9}$$

where k_1 is the air turbine damping coefficient.

Combining (8) and (9) gives

$$\frac{\rho_0 V}{\gamma p_0}\dot{p} + \rho_0\left(1 + \frac{p}{\gamma p_0}\right)\dot{V} + \frac{p}{k_1} = 0. \tag{10}$$

Equation (10) is the dynamic equation for the air chamber volume and the chamber pressure forming a closed dynamic system because of the application of the PTO. If the chamber volume is known (for example, the internal water surface motion is known), then the chamber pressure can be resolved for a given PTO, and vice versa.

D. Nonlinear PTO$_1$ (Impulse turbines)

For an orifice PTO (model scale) or an impulse turbine PTO (full scale device), the general relation of the chamber pressure and the mass flowrate through the PTO is a parabolic relation, and the mathematical expressions are as follows:

For the exhalation process

$$p = k_2 \dot{m}^2, \tag{11}$$

where k_2 is the mass flowrate damping coefficient, or

$$\dot{m} = -\sqrt{\frac{p}{k_2}}. \tag{12}$$

For the inhalation process

$$p = -k_2 \dot{m}^2 \tag{13}$$

or

$$\dot{m} = \sqrt{\frac{-p}{k_2}}. \tag{14}$$

The corresponding thermodynamic equations are:

For exhalation

$$\frac{\rho_0 V}{\gamma p_0}\dot{p} + \rho_0\left(1 + \frac{p}{\gamma p_0}\right)\dot{V} + \sqrt{\frac{p}{k_2}} = 0. \tag{15}$$

For inhalation

$$\frac{\rho_0 V}{\gamma p_0}\dot{p} + \rho_0\left(1 + \frac{p}{\gamma p_0}\right)\dot{V} - \sqrt{\frac{-p}{k_2}} = 0. \tag{16}$$

Similar to the linear air turbine PTO, by Eqs. (15) and (16), the air chamber volume and the chamber pressure have been dynamically linked together in a closed dynamic system form.

For a more general nonlinear air turbine (see Sheng *et al.*[11]), it may be difficult to represent its PTO as a purely linear or parabolic PTO. Generally, a polynomial expression can fit better for the relation of the pressure and mass flowrate for most air turbines, and the linear and the

orifice PTO can be taken as the specific cases when k_2 or k_1 is taken as a very small value in the following formulas correspondingly.

In exhalation,

$$p = -k_1\dot{m} + k_2\dot{m}^2, \tag{17}$$

where k_1 and k_2 are the damping coefficients corresponding to the linear and nonlinear part.

So,

$$\dot{m} = \frac{k_1 - \sqrt{k_1^2 + 4k_2p}}{2k_2}. \tag{18}$$

In inhalation,

$$p = -k_1\dot{m} - k_2\dot{m}^2, \tag{19}$$

or

$$\dot{m} = \frac{-k_1 + \sqrt{k_1^2 - 4k_2p}}{2k_2}. \tag{20}$$

Hence, the corresponding thermodynamic equations would be given as follows:
For exhalation

$$\frac{\rho_0 V}{\gamma p_0}\dot{p} + \rho_0\left(1 + \frac{p}{\gamma p_0}\right)\dot{V} - \frac{k_1 - \sqrt{k_1^2 + 4k_2p}}{2k_2} = 0; \tag{21}$$

for inhalation

$$\frac{\rho_0 V}{\gamma p_0}\dot{p} + \rho_0\left(1 + \frac{p}{\gamma p_0}\right)\dot{V} - \frac{-k_1 + \sqrt{k_1^2 - 4k_2p}}{2k_2} = 0. \tag{22}$$

E. Nonlinear PTO$_2$ (Bi-radial turbines)

A novel air turbine has been recently developed by Falcao *et al.*[6,12] This type of air turbine is a nonlinear PTO, but the relation of the chamber pressure and the mass flowrate has a very different form (see Falcao *et al.*[6]).

In the exhalation process

$$p = k_3\sqrt{-\dot{m}}, \tag{23}$$

where k_3 is the PTO damping coefficient.

So,

$$\dot{m} = -\left(\frac{p}{k_3}\right)^2. \tag{24}$$

In the inhalation process

$$p = -k_3\sqrt{\dot{m}}, \tag{25}$$

hence,

$$\dot{m} = \left(\frac{p}{k_3}\right)^2. \tag{26}$$

The corresponding thermodynamic equations are:
For exhalation

$$\frac{dV}{dt}+\frac{V}{\gamma p_0+p}\frac{dp}{dt}+\left(\frac{p}{k_3}\right)^2=0, \tag{27}$$

for inhalation

$$\left(1+\frac{p}{\gamma p_0}\right)\frac{dV}{dt}+\frac{V}{\gamma p_0}\frac{dp}{dt}-\left(\frac{p}{k_3}\right)^2=0. \tag{28}$$

For more general cases of this type of the air turbine, the PTO relation can be represented in two terms: linear term and nonlinear term.

Similarly, in the exhalation process

$$p=-k_1\dot{m}+k_3\sqrt{-\dot{m}}, \tag{29}$$

the corresponding mass flowrate is

$$\dot{m}=-\left(\frac{p}{k_1}+\frac{k_3^2}{2k_1^2}-\frac{k_3}{2k_1^2}\sqrt{k_3^2+4k_1p}\right), \tag{30}$$

in the inhalation process

$$p=-k_1\dot{m}-k_3\sqrt{\dot{m}}. \tag{31}$$

So,

$$\dot{m}=\frac{k_3^2}{2k_1^2}-\frac{p}{k_1}-\frac{k_3}{2k_1^2}\sqrt{k_3^2-4k_1p}. \tag{32}$$

The corresponding thermodynamic equations are:
For exhalation

$$\frac{\rho_0 V}{\gamma p_0}\dot{p}+\rho_0\left(1+\frac{p}{\gamma p_0}\right)\dot{V}+\frac{p}{k_1}+\frac{k_3^2}{2k_1^2}-\frac{k_3}{2k_1^2}\sqrt{k_3^2+4k_1p}=0; \tag{33}$$

for inhalation

$$\frac{\rho_0 V}{\gamma p_0}\dot{p}+\rho_0\left(1+\frac{p}{\gamma p_0}\right)\dot{V}+\frac{p}{k_1}-\frac{k_3^2}{2k_1^2}+\frac{k_3}{2k_1^2}\sqrt{k_3^2-4k_1p}=0. \tag{34}$$

III. EXPERIMENTAL VALIDATION OF AIR COMPRESSIBILITY

To validate the air compressibility in the chamber, a test rig has been used to study the air compressibility in the air chamber when a PTO, such as an orifice PTO, is applied. The piston of a diameter 0.30 m is designed to represent the air chamber for an OWC device which is driven by a powerful electric motor (see Figures 2 and 3). On the top of the cylinder, an orifice (Figure 2) or an extension for accommodating the porous materials (Figures 3 and 4) is mounted. The well-controlled electric motor can drive the piston according to the pre-set motions. For example, in a sinusoidal test, the pre-set amplitude and frequency for the piston can be easily achieved. In the test, the chamber pressure is measured under the pre-set drive of the piston.

For a model test OWC device of a similar size, the wave tank would generate a power of about 1 W, but the electric motor could provide a much higher input power (more than 100 W) to the piston so that the air compressibility can be generated easily in the air chamber in the rig test.

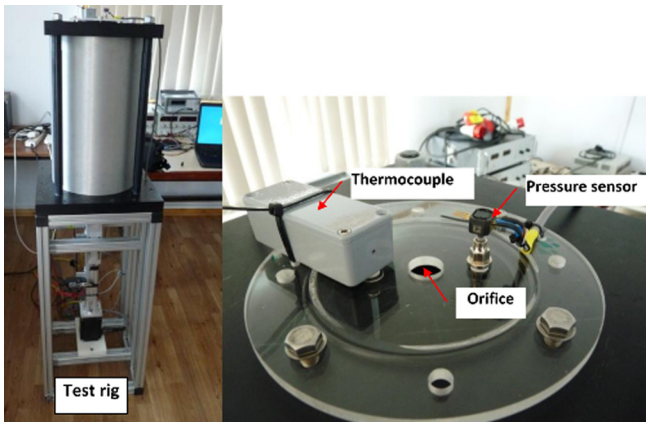

FIG. 2. Orifice PTO test on the test rig.

Figure 5 shows the test result for an orifice PTO for the piston. In the test, an orifice of 0.019 m is used, which represents 0.4% to the piston area. Under the pre-set piston motion of an amplitude 0.04 m and frequency 1 Hz, the air compressibility can be obviously observed (the hysteresis loop in the chamber pressure and the air volume changing rate, $\dot{V} = \frac{dV}{dt}$). If there is no air compressibility, the air volume changing rate will be the same as the volume flowrate passing the PTO, and the relation between the chamber pressure and volume changing rate would be determined by the PTO relation which is shown in the single curve identified as 'incompressible' in Figure 5.

From the comparison, it can be seen that the numerical method has well predicted the air compressibility in the air chamber. In another example, the piston motion amplitude is much reduced to 0.012 m, but the frequency is increased to 1.44 (Figure 6), in which the chamber

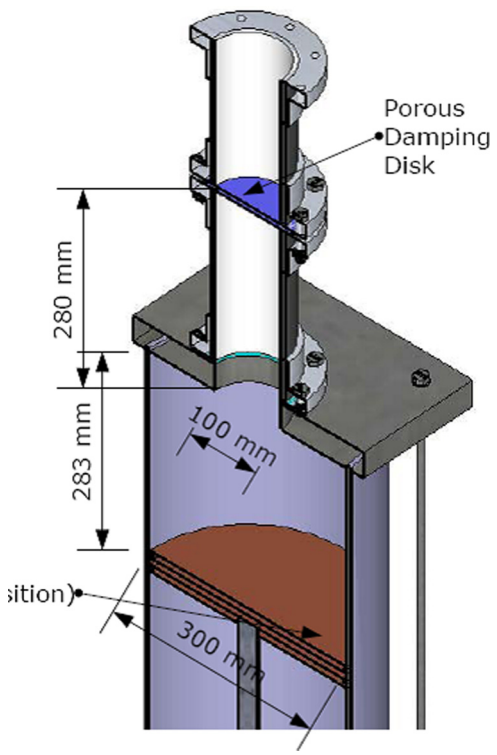

FIG. 3. A schematic drawing of the porous membrane tested as a PTO damping material.

FIG. 4. Porous damping disk for representing linear air flow damping.

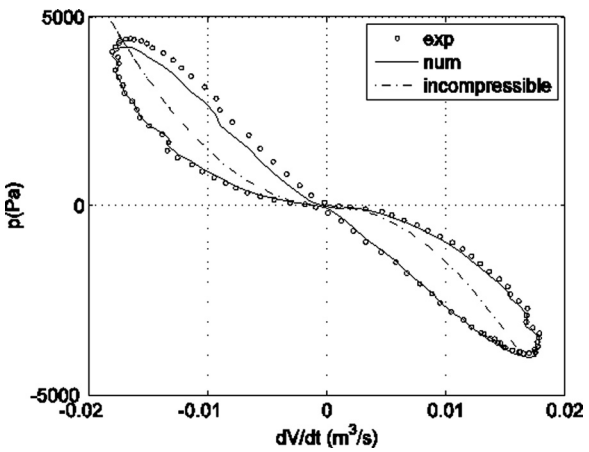

FIG. 5. Comparison of chamber pressure and mass flow rate (numerical against measured data), orifice diameter $\varphi = 0.019$ m, piston motion: A = 0.040 m, f = 1.00 Hz).

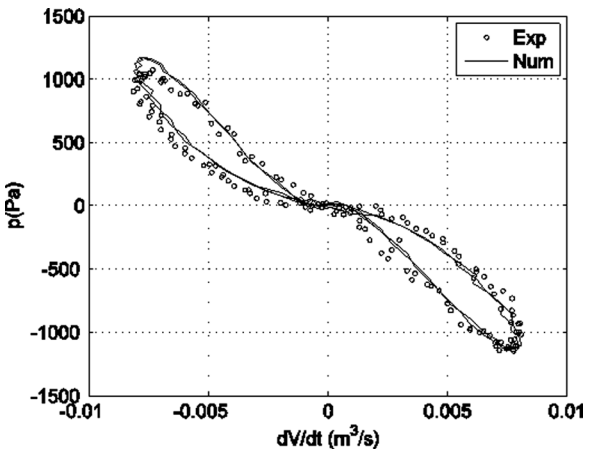

FIG. 6. Comparison of chamber pressure and mass flow rate (numerical against measured data), orifice diameter $\varphi = 0.019$ m, piston motion: A = 0.012 m, f = 1.44 Hz).

pressure and the air volume changing rate are much smaller than the previous case, but the air compressibility is still seen obviously. And again, the numerical method predicts the air compressibility well.

In scale models, the porous membranes (Figure 4) have been used to approximate the linear air turbine PTO (see details in Sheng *et al.*[11]). Practically, a weak nonlinear relation between the chamber pressure and the air volume changing rate can be seen (Figure 7). Hence, a polynomial relation (Eqs. (17) and (19)) between the chamber pressure and the flowrate would be a better choice. Using a polynomial relation, the numerical result shows a close agreement to the experimental data (Figure 7).

IV. OWC WAVE ENERGY CONVERSION

For large OWC wave energy converters, nonlinear effects may be more evident, due to the possible large amplitude motions of the converters, or due to the nonlinear PTO or nonlinear mooring forces involved in the dynamic system. In this regard, time-domain analysis is normally conducted. As a follow-up to the research work in the first part where the hydrodynamic model has been extensively studied and built (Sheng *et al.*[14]), in this part, the hydrodynamic model and the thermodynamic model is coupled together to form an entire dynamic system for OWC wave energy converters.

In the first part of the research, hydrodynamically, an OWC wave energy converter can be represented by two interacting bodies: the actual floating structure which represents the device itself and an imaginary piston representing the water body in the water column. By applying an air turbine PTO, the relative motion between the two bodies create a varying volume in the chamber, which could induce a changing chamber pressure, driving the air out of or sucking the air into the air chamber though the PTO system. Due to a relatively small air passage in the PTO, the air is normally accelerated in speed by 50–150 times. This very much accelerated air flow through the air turbine PTO could drive the air turbine in a high rotating speed, in a way that the pneumatic energy is converted into mechanic energy. When the internal water surface moves up, or the device structure moves down, the volume of the air chamber becomes smaller, which could create a positive pressure in the air chamber. The positive chamber pressure will drive the air out of the air chamber, and at the same time, it will push the device structure upward and the internal water surface downward so that the air volume will be enlarged. The reduced air in the air chamber and the consequences of the dynamic motions of the device and the piston will have a trend to increase the air volume, so the dynamic system is stable.

To simplify the analysis, we assume only the heave motions of the two bodies can be used to convert the wave energy into pneumatic energy, because the heave motions may not be coupled with any other types of motions when an axi-symmetrical OWC is considered.

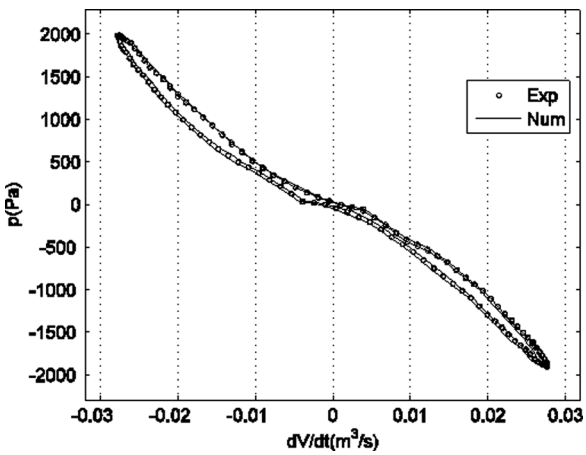

FIG. 7. Comparison of chamber pressure and mass flow rate (numerical against measured data), porous materials: 1 brown and 1 blue, piston motion: A = 0.075 m, f = 0.833 Hz).

Followed the convention used in the first part of the research (Sheng *et al.*[14]), the two-body system of the OWC device would be noted by the following motion modes: x_i, $(i=1,\ldots,6)$ for the 6-DOF motions for the device structure, and x_i $(i=7,\ldots,12)$ for the 6-DOF motions for the imaginary piston. Hence x_3 and x_9 would be the heave motions for the two bodies, respectively. The coupled hydrodynamic-thermodynamic equation would be

$$[m_{33}+A_{33}(\infty)]\ddot{x}_3(t)+\int_0^t K_{33}(t-\tau)\dot{x}_3(\tau)d\tau+C_{33}x_3(t)+A_{39}(\infty)\ddot{x}_9(t)+\int_0^t K_{39}(t-\tau)\dot{x}_9(\tau)d\tau+C_{39}x_9(t)=F_3(t)+A_0p, \tag{35}$$

$$A_{93}(\infty)\ddot{x}_3(t)+\int_0^t K_{93}(t-\tau)\dot{x}_3(\tau)d\tau+C_{93}x_3(t)+[m_{99}+A_{99}(\infty)]\ddot{x}_9(t)+\int_0^t K_{99}(t-\tau)\dot{x}_9(\tau)d\tau+C_{99}x_9(t)=F_9(t)-A_0p, \tag{36}$$

where A_0 the sectional area of the water column.

In the time domain equations, the hydrodynamics of the device and the piston have been modified by the chamber pressure, which is the solution of the thermodynamic equations, for example, Eq. (15) or Eq. (16). And due to the motions, the air volume is calculated by the following relation:

$$V(t)=V_0-A_0[x_9(t)-x_3(t)], \tag{37}$$

where $V(t)$ is the time dependent chamber air volume, and V_0 the air volume when the device is in calm water.

So far, we have four unknowns: x_3, x_9, p, and V, and we have four equations for solving them:

- Two coupled hydro-thermodynamic equations (35) and (36);
- One thermodynamic equation, which may be different for a different PTO. For example, for the linear PTO, it would be Eq. (10);
- The relation of the motions and the air volume, given by Eq. (37).

As a specific case, when the OWC is bottom-fixed on the seabed, then the coupled hydro-thermodynamic equation would be reduced to

$$[m_{99}+A_{99}(\infty)]\ddot{x}_9(t)+\int_0^t K_{99}(t-\tau)\dot{x}_9(\tau)d\tau+C_{99}x_9(t)=F_9(t)-A_0p, \tag{38}$$

and

$$V(t)=V_0-A_0x_9(t). \tag{39}$$

In the case of the bottom-fixed OWC, there are three unknowns and three equations.

V. PRIMARY WAVE ENERGY CONVERSION

After solving the coupled time-domain equations, we can assess the performance of the wave energy converters, including the wave energy conversion and motion responses.

The power converted by the OWC device can be calculated,

$$P(t)=p(t)\dot{m}(t)/\rho_{ref}, \tag{40}$$

where $P(t)$ is the converted power, ρ_{ref} the reference density of air passing through the PTO, which is chosen when calibrating the PTO. Normally, it can be taken as the atmospheric density.

The averaged capture power is

$$\bar{P} = \frac{1}{T\rho_{ref}} \int_0^T p(t)\dot{m}(t)dt, \tag{41}$$

where T is the time interval for calculating the averaged power.

The wave energy capture width can be calculated as

$$W = \frac{\bar{P}}{E_{wave}}, \tag{42}$$

where E_{wave} is the wave energy flux per unit wave front. For regular waves in deep water,

$$E_{wave} = \frac{\rho_w g^2}{32\pi} H^2 T, \tag{43}$$

where ρ_w is water density, g the gravity acceleration, H the wave height and T the wave period.

And for irregular waves in deep water,

$$E_{wave} = \frac{\rho_w g^2}{64\pi} H_s^2 T_e, \tag{44}$$

where H_s is the significant wave height and T_e the wave energy period.

The efficiency of the wave energy conversion is given by

$$\eta = \frac{W}{B} \tag{45}$$

where B is the width of the OWC device.

The motion response in regular waves can be easily calculated as

$$X = \frac{x_{peak} - x_{trough}}{H}, \tag{46}$$

where x_{peak} and x_{trough} are the motion peak and trough values in regular waves, and H is the wave height.

The chamber pressure response in regular waves is defined as

$$p_{res} = \frac{p_{peak} - p_{trough}}{H}, \tag{47}$$

where p_{peak} and p_{trough} are the chamber pressure peak and trough values in regular waves (note: the chamber pressure may not be fully sinusoidal if a nonlinear PTO is applied, see the examples in Sec. VI).

The captured power response is calculated as

$$P_{res} = \frac{\bar{P}}{H^2}. \tag{48}$$

VI. RESULT ANALYSIS

A. Fixed OWC (OWC_1)

The first generic OWC is a bottom-fixed OWC, see Figure 8. The OWC has a very simple structure, essentially a circular cylinder with a co-axial circular cylinder moonpool. The OWC device has an outside diameter of 0.316 m, and an inside diameter of 0.104 m (i.e., the

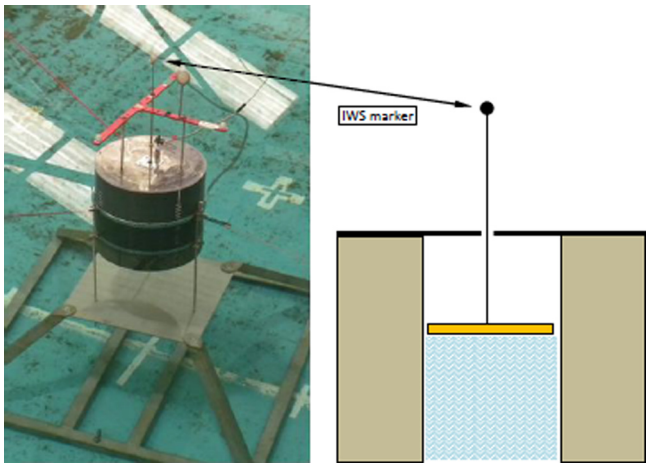

FIG. 8. Bottom-fixed OWC model tested in a wave tank.

moonpool diameter). On top of the moonpool, a small orifice can be mounted for modelling an impulse-type air turbine PTO.

The overall length of the OWC model is 0.4 m, of which 0.3 m is immersed in water. The OWC has been well ballasted though it is a bottom-fixed OWC. The OWC has been fixed using three small rods on a frame which is in turn fixed on the tank floor (Figure 8). The fixed frame is designed to have small influence on the OWC internal water surface motion. So the OWC could be considered as being isolated well, and it was hoped that its hydrodynamic analysis could be simple, similar to the solutions of Mavrakos *et al.*[15] and Martins-rivas *et al.*[16] However, in this research, a commercial BEM code WAMIT is employed because of its popularity and its capability in dealing with complicated geometries.

Figures 9 and 10 show the comparisons of the internal water surface motion and the chamber pressure in a regular wave of $H = 40$ mm and $T = 1.2$ s. In the test, an orifice of 12 mm has been used to model a nonlinear PTO. It can be seen from the comparisons that the numerical model developed in this research has well predicted the IWS motion and the chamber pressure.

It is also needed to point out that in the numerical simulation, all hydrodynamic parameters are from WAMIT assessment. For instance, no additional damping is required, though the other form damping may be present (rather than the only hydrodynamic damping in the WAMIT analysis). However, the numerical simulation shows that in the bottom-fixed OWC, the orifice has applied an appropriate damper to the internal water surface motion so that the numerical prediction is very close to the experimental data. It can be concluded that the damping of the internal water surface motion for the fixed OWC device is dominated by the damping from the PTO, though WAMIT under-predicts the hydrodynamic damping (also see the first part of research, Sheng *et al.*[14]).

Another interesting fact is that by applying a nonlinear PTO (an orifice PTO in this case), the internal water surface motion is dominated by the wave frequency response (Figure 9), but

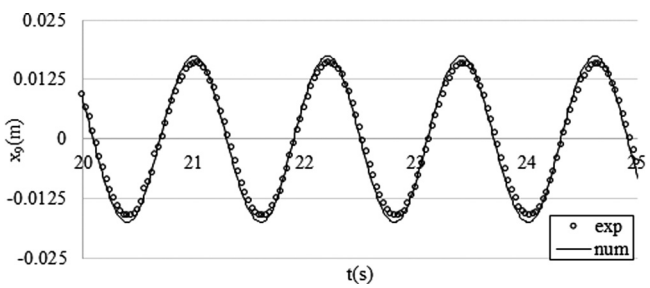

FIG. 9. Comparison of the relative motion in the fixed OWC (H = 40 mm, T = 1.2 s, $\varphi = 12$ mm).

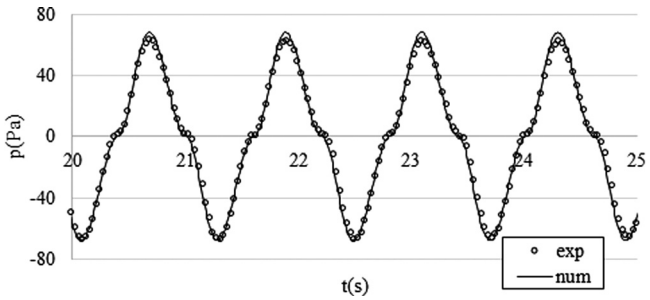

FIG. 10. Comparison of the chamber pressures (H = 40 mm, T = 1.2 s, φ = 12 mm).

the chamber pressure has an obvious dead band around zero chamber pressure. Hence, as pointed out previously, the chamber pressure in this case may not be modelled appropriately using the linear methods because it contains the components of both the wave frequency and higher frequency in regular waves.

Figures 11–13 show the response comparisons of the internal water surface motion, chamber pressure, and the capture power. It can be seen that the numerical method has again well predicted all the responses when they are compared to the experimental data.

Figures 14 and 15 show the power capture width and the wave energy conversion efficiency of the fixed OWC in regular waves. It can be seen that the OWC has a very low wave energy conversion capacity, and the maximum energy conversion efficiency is about 3.5%. The relatively small water column in the OWC is a main factor for this low figure. It is no surprise since the OWC is not designed to have a good energy conversion efficiency, but a simple structure.

Similar results can be seen in the case of an orifice of 14 mm, see Figures 16–19. Again the numerical predictions are very close to the experimental data. Though a higher maximal energy conversion efficiency can be seen (about 4.5%, Figure 19), its energy capture bandwidth is narrowed.

From the examples, it can be seen that the generic OWC has a very low wave energy conversion efficiency (the maximal energy conversion efficiency is less than 5%). This is understandable because the OWC device is only designed to have a simple structure, rather than an optimised shape for wave energy conversion. To have a good wave energy conversion efficiency, the OWC must be designed to have a large water column (see Sheng *et al.*[17]). In this case, the water column is very small (less than 1/3 of the overall diameter). Besides, the OWC has a long water column, the maximal energy conversion efficiency happens in a longer period, which would make the conversion efficiency smaller.

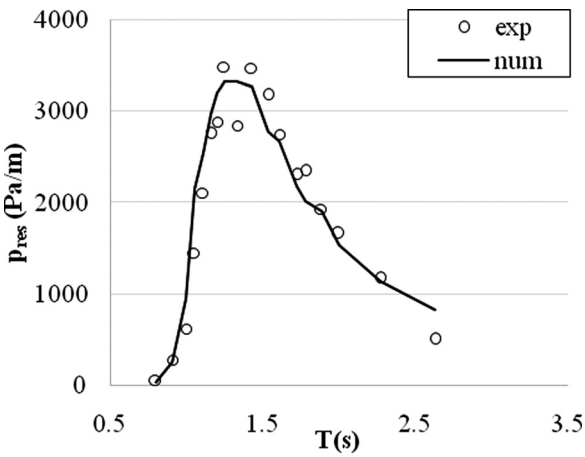

FIG. 11. Responses of chamber pressure in regular waves (φ = 12 mm, H = 40 mm).

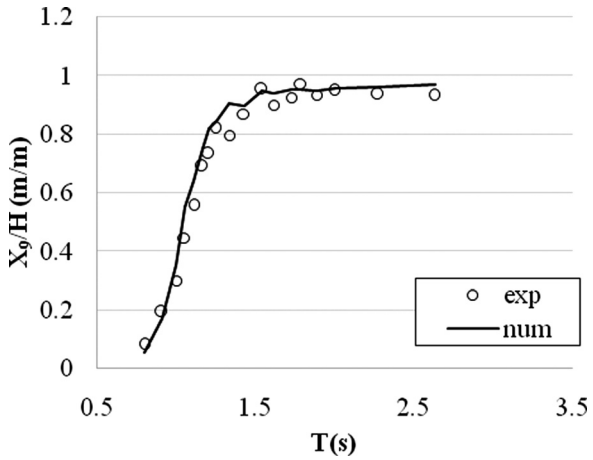

FIG. 12. Responses of internal free surface in regular waves ($\varphi = 12$ mm, H = 40 mm).

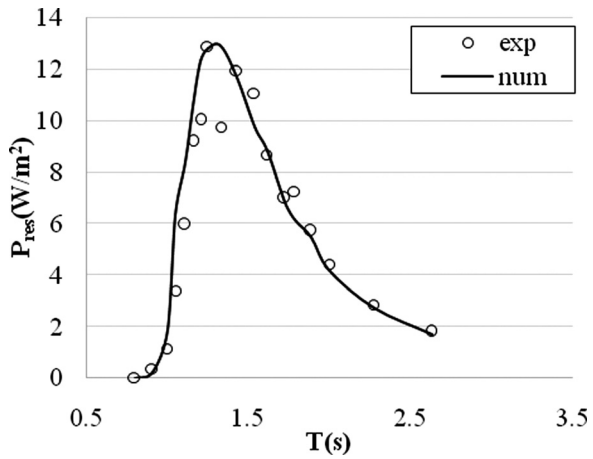

FIG. 13. Capture power response in regular waves ($\varphi = 12$ mm, H = 40 mm).

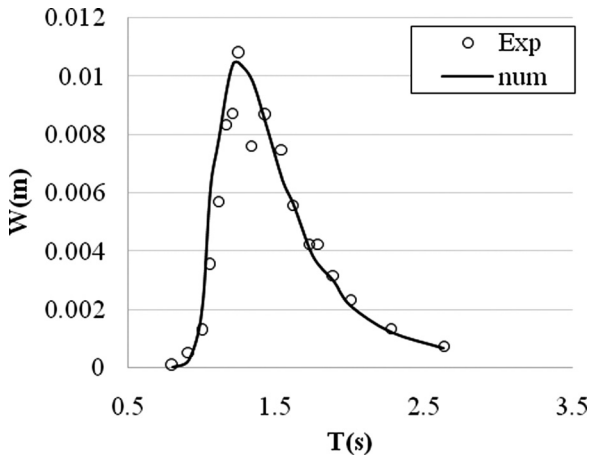

FIG. 14. Capture width in regular waves ($\varphi = 12$ mm, H = 40 mm).

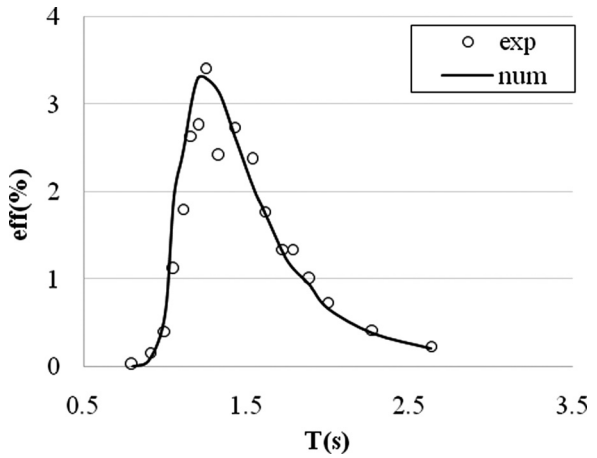

FIG. 15. Wave energy conversion efficiency in regular waves ($\varphi = 12$ mm, H = 40 mm).

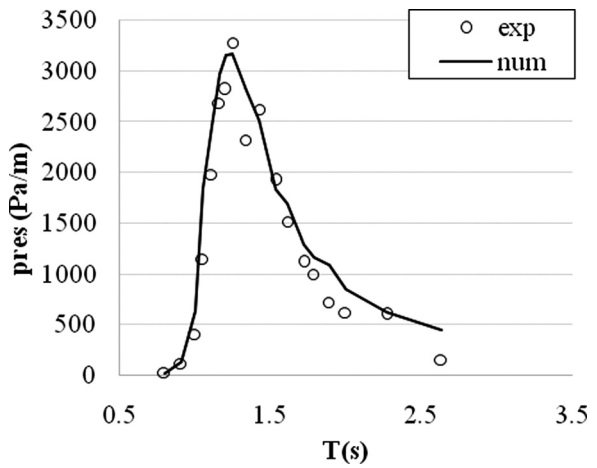

FIG. 16. Responses of chamber pressure in regular waves ($\varphi = 14$ mm, H = 40 mm).

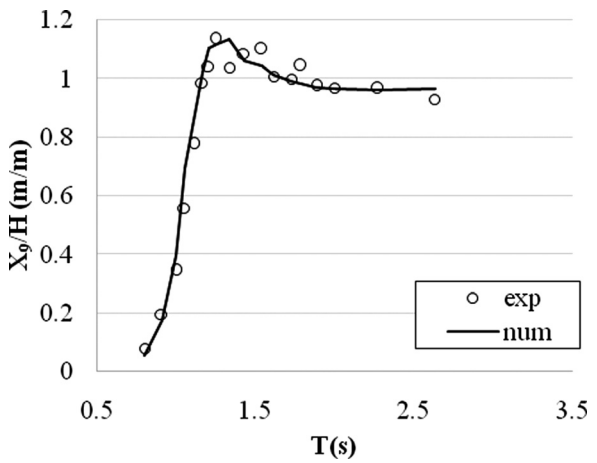

FIG. 17. Responses of internal free surface in regular waves ($\varphi = 14$ mm, H = 40 mm).

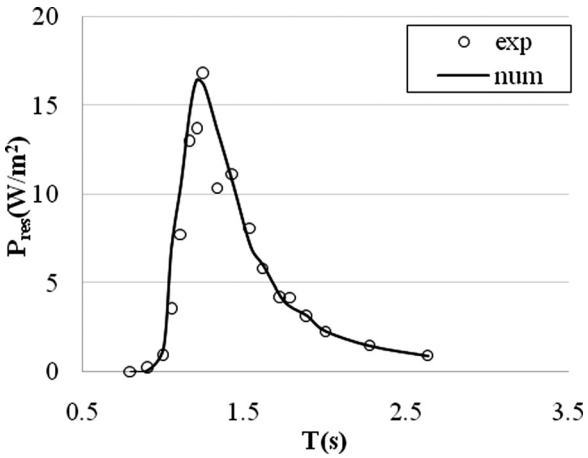

FIG. 18. Capture power response in regular waves ($\varphi = 12$ mm, H = 40 mm).

B. Floating OWC (OWC$_2$)

The second generic OWC is a floating cylindrical OWC, which has been studied in the first part of the research (Sheng *et al.*[14]). Figure 20 shows its sectional dimensions of the generic OWC device, and Figure 21—a drawing of the floating OWC and the mooring system. Three catenary chains were used for mooring the device in the tank during the test. The OWC has a cylindrical water column of a diameter 0.23 m, and draft 0.15 m. Outside the water column, the foam float of a thickness 0.04 m and overall length of 0.20 m (0.10 m is immersed in water in calm water). The OWC has a mass of 3.39 kg.

In the test, the mooring system has been assumed to have only a small influence to the motions of the floating OWC. Hence, in the analysis, the mooring forces are not included.

Figure 22 shows the heave responses of the device and the piston, and their relative motion (internal water surface motion) from numerical prediction. In the case of no additional damping, the heave responses of the device and the piston are large (maximal value more than 5.0). Due to the difference of the resonance periods between the device and the piston, the internal water surface response ('solid line' in Figure 22) has two peaks at periods of $T = 0.74$ s and $T = 0.935$ s, respectively. The first peak corresponds to the device heave natural period, and the second peak to the piston heave natural period.

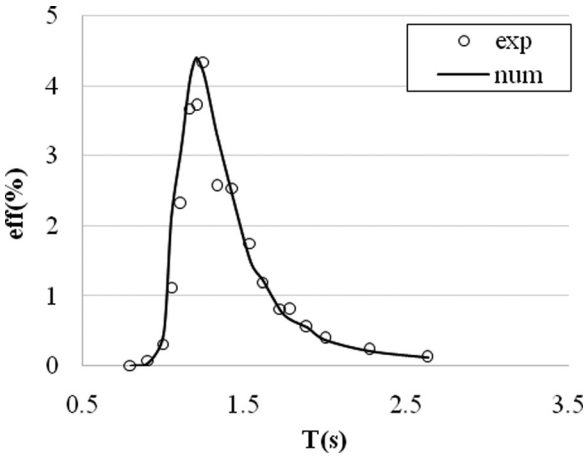

FIG. 19. Wave energy conversion efficiency in regular waves ($\varphi = 14$ mm, H = 40 mm).

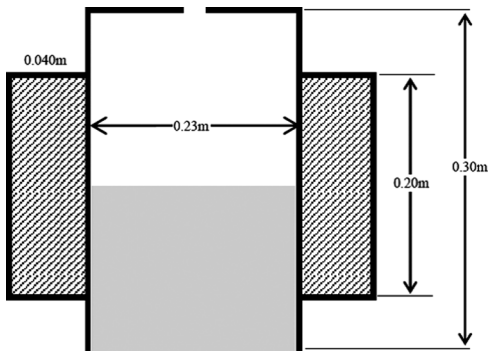

FIG. 20. The second generic OWC_2 (a floating OWC).

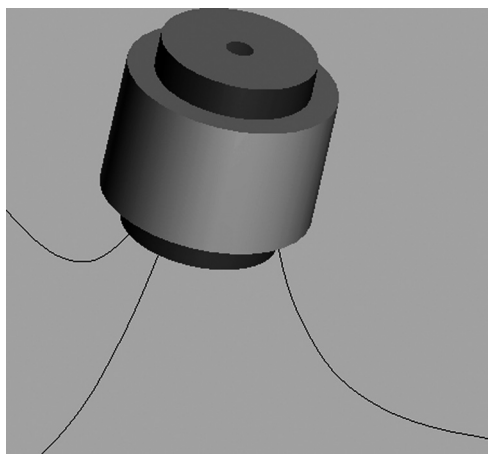

FIG. 21. OWC_2 and mooring system in the tank test.

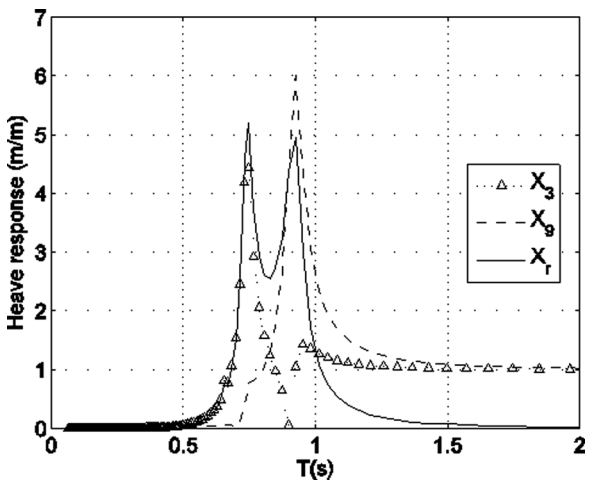

FIG. 22. Heave responses of the two bodies and the internal water surface for the case of no added damping and PTO damping.

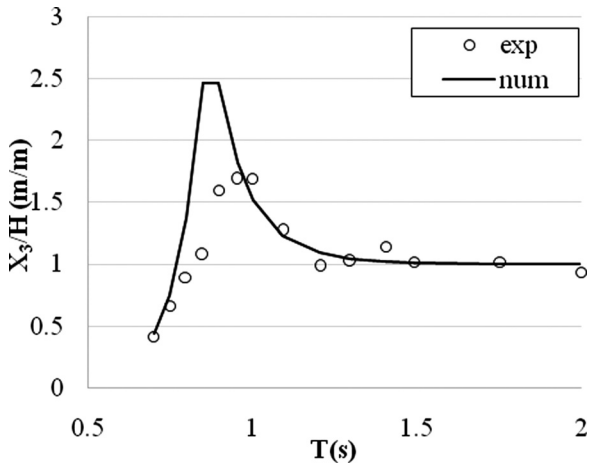

FIG. 23. Heave motion response of the device structure ($\varphi = 22$ mm, H = 40 mm).

Case 1: Zero additional damping

In the first case of the numerical assessment for the floating OWC device, no additional damping is applied to the motions of the floating device and the piston. Hence, in the dynamic system of the numerical analysis, the damping coefficients included for analysis are only from the hydrodynamic radiation damping and the PTO damping due to the application of an orifice PTO. Figure 23 shows the heave response of the device, in which the numerical method has overpredicted the heave motion of the device. It can be understood that the ignorance of the other type of damping for the heave motion, such as viscous damping, has caused the problem. From Figure 24, it can be seen that the internal water surface has been slightly under-predicted whilst the chamber pressure response is overpredicted. The reason for this is mainly due to the overpredicted heave motion for the device!

Because of the overpredicted chamber pressure, the power capture response and, therefore, the power capture width and the power conversion efficiency are all overpredicted (Figures 25–28).

Case 2: added damping for structure heave motion ($B_{33} = 5$ Ns/m)

From the example above, the ignorance of the damping for the device heave motion has especially overpredicted the heave motion of the device, and as a result of that, the OWC performance has generally been over-predicted. In the next case, the heave motion of the device is supposed to be damped by including some additional damping ($B_{33} = 5$ Ns/m) so that the device heave motion can be more rightly assessed. Figure 29 shows a significant reduction in the

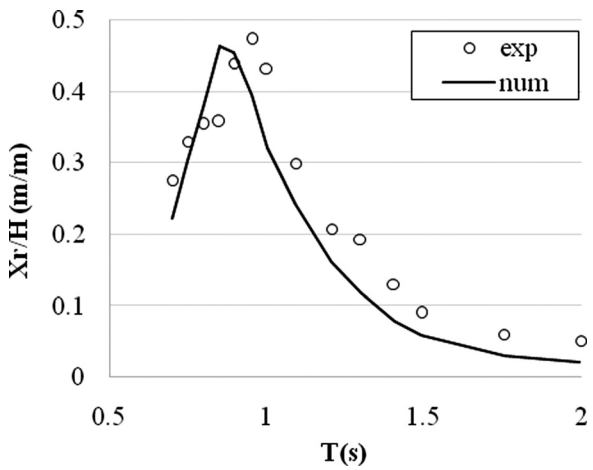

FIG. 24. IWS motion response ($\varphi = 22$ mm, H = 40 mm).

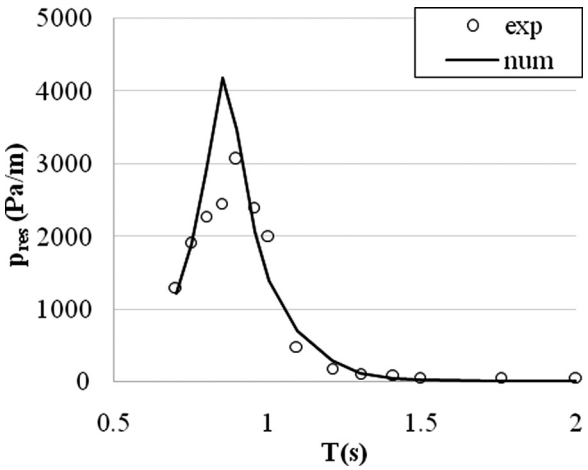

FIG. 25. Chamber pressure response ($\varphi = 22$ mm, H = 40 mm).

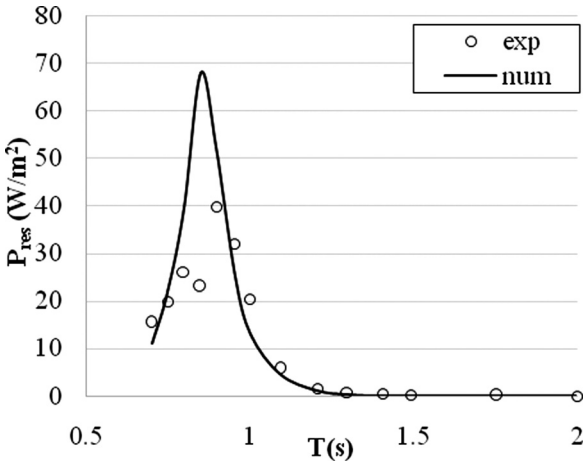

FIG. 26. Capture power response ($\varphi = 22$ mm, H = 40 mm).

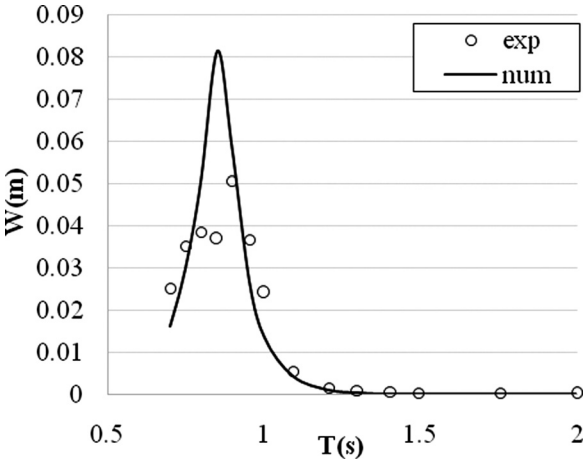

FIG. 27. Power capture width ($\varphi = 22$ mm, H = 40 mm).

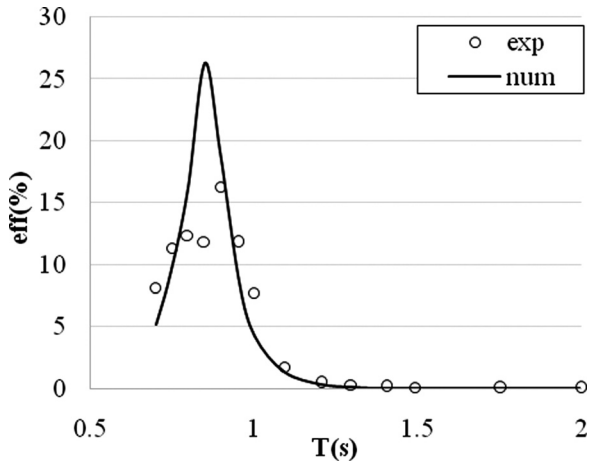

FIG. 28. Power conversion efficiency ($\varphi = 22$ mm, H = 40 mm).

device heave response (X_3) due to the additional damping (no PTO damping yet). The maximal response of the heave motion is now slightly larger than 1 (much smaller than in the undamped case, compared to Figure 22). Due to the appropriate prediction in the device heave motion, the response of the internal water surface is now more affected by the piston motion, hence a single peak can be only seen.

In the case of OWC wave energy conversion with an orifice PTO, with the additional damping coefficient applied to the device heave motion, the device heave response can be now well reproduced (see Figure 30). As a result of this, the chamber pressure and the power capture are all well predicted (see Figures 31–34) though the internal water surface motion is slightly underpredicted (Figure 35). Hence, it can be concluded that for a floating OWC device, if the device heave motion can be well predicted, the power conversion performance will be correctly assessed. Again, from the numerical simulation, it is shown that the OWC performance can be well assessed and it is not necessary to apply any additional damping to the piston heave motion. This is a same conclusion as we have drawn for the bottom-fixed OWC in which the heave motion is only zero.

From the examples of two generic OWC devices, the maximal energy conversion efficiency of the second OWC is much higher than the first generic OWC (15% vs. 4.5%), even though the second OWC is much lighter than the first OWC (3.39 kg vs. 20.98 kg). The main reason for this is the sizes of the OWC water columns (see Sheng *et al.*[17]): the water column of the

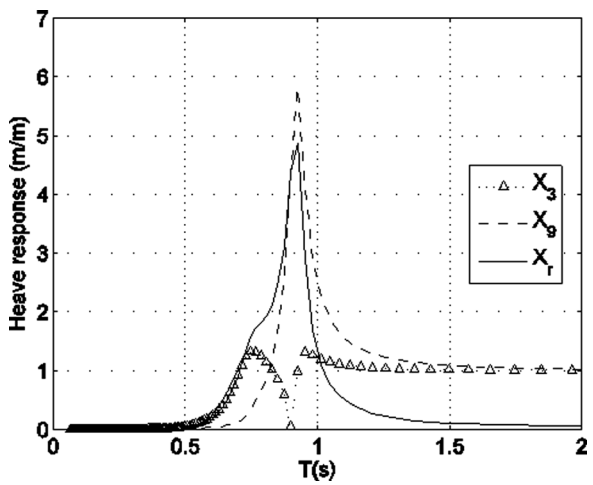

FIG. 29. Heave responses of the two bodies (added damping, $B_{33} = 5$ Ns/m).

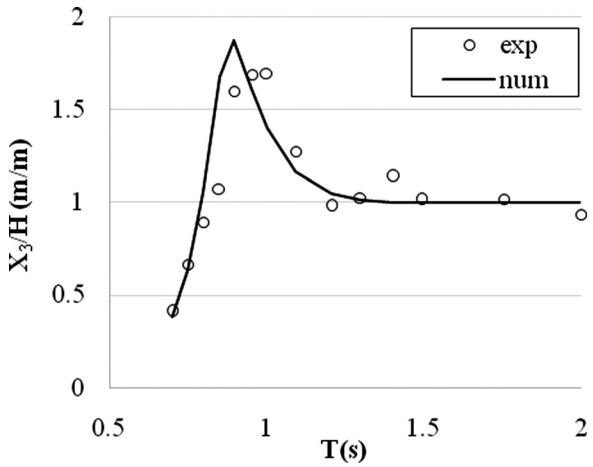

FIG. 30. Heave motion response of the device ($\varphi = 22$ mm, H = 40 mm).

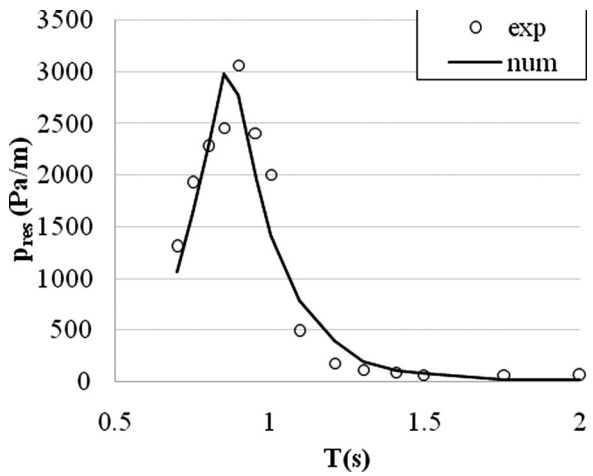

FIG. 31. Chamber pressure response ($\varphi = 22$ mm, H = 40 mm).

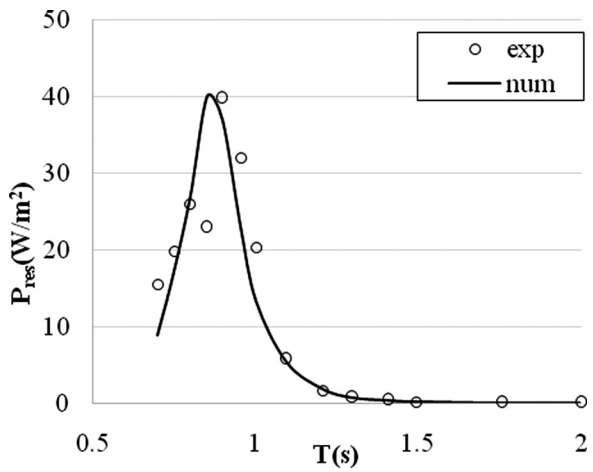

FIG. 32. Capture power response ($\varphi = 22$ mm, H = 40 mm).

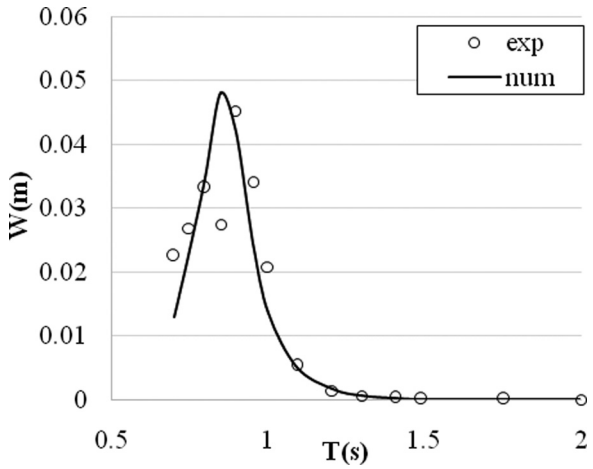

FIG. 33. Power capture width ($\varphi = 22$ mm, H = 40 mm).

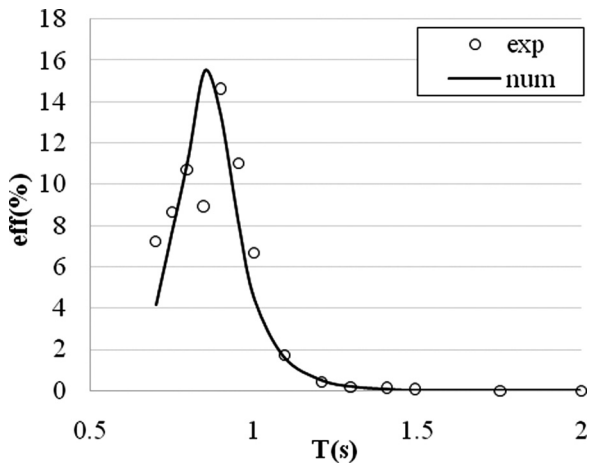

FIG. 34. Power conversion efficiency ($\varphi = 22$ mm, H = 40 mm).

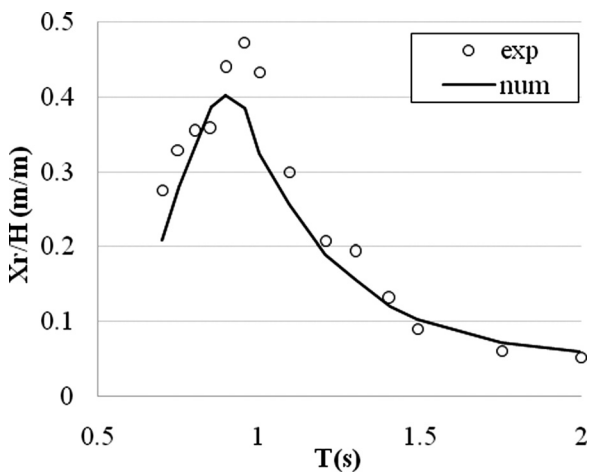

FIG. 35. IWS motion response ($\varphi = 22$ mm, H = 40 mm).

second OWC is about 4 times of the first OWC (maximal efficiency is about 3.33 times for reference). In addition, for the first OWC, the maximal energy conversion happens at a longer wave period (1.17 s against 0.935 s), which will inherently make the energy conversion efficiency smaller.

VII. CONCLUSIONS

In developing a full numerical assessment method for OWC wave energy converters, the detailed thermodynamics of the air flow through the PTO has been presented, and relevant validations have been made with the experimental data for a nonlinear orifice PTO and a linear porous membrane PTO. By coupling the hydrodynamics of the OWC (following the hydrodynamic assessment carried out in the first part of the research) and the thermodynamics presented in this part of the research, a time domain dynamic equation for the OWC device can be established, through the interaction of the chamber pressure and the air chamber volume. Solving the time-domain equation, the performance of the OWC can be assessed further, such as the power capture capacity, curve, width and efficiency. The numerical simulations have been made for two different generic OWCs: bottom-fixed and floating. From the comparisons to the experimental data, it is shown that the developed numerical method is very capable of assessing the performance of the OWC wave energy converters.

From the research and the examples, following conclusions can be drawn:

- The time-domain equation is fully established for the OWC performance assessment, including the thermodynamics of the air in the chamber due to the application of the PTOs and its coupling with the hydrodynamic motions of the device and the piston.
- The thermodynamic equation detailed in the research can be used for predicting the chamber pressure and the air flow through the PTO, including the air compressibility. The comparison to the experimental data has shown its suitability for the compressible air.
- If a nonlinear PTO is used, such as the orifice PTO in the example, under the excitation of regular waves, the internal water surface motion has been dominated by the components of wave frequency. In contrast, the chamber pressure has shown the dependencies on both wave frequency and high frequencies, which is an indicator of a strong nonlinearity. This fact could imply that in the hydrodynamic module, the internal water surface motion should be assessed rather than the chamber pressure which would be a solution of the thermodynamic equation, as shown in the research work.
- For the bottom-fixed OWC, the numerical assessment can be straightforward. The hydrodynamic damping (assessed in WAMIT) and the PTO damping appear accurate enough for the OWC performance assessment.
- For the floating OWC, the device motion can play an important role in the wave energy conversion, hence it is critical if the motion prediction can be appropriately carried out. The OWC performance assessment can be reliable only if the device motion can be well reproduced.

ACKNOWLEDGMENTS

This material is based upon works supported by the Science Foundation Ireland (SFI) under the Charles Parsons Award at Beaufort Research-Hydraulics and Maritime Research Centre (HMRC), University College Cork, Ireland. Statistics and data were correct at the time of writing the article, however, the authors wish to disclaim any responsibility for any inaccuracies that may arise.

[1]A. F. d. O. Falcao and P. A. P. Justino, "OWC wave energy devices with air flow control," Ocean Eng. **26**, 1275–1295 (1999).
[2]J. Weber, "Representation of non-linear aero-thermodynamics effects during small scale physical modelling of OWC WECs," Proceedings of the 7th European Wave and Tidal Energy Conference, 11–14th September 2007, Porto, Portugal.
[3]W. Sheng, R. Alcorn, and A. Lewis, "Physical modelling of wave energy converters," Ocean Eng. **84**, 29–36 (2014).
[4]A. J. N. A. Sarmento, L. M. C. Gato, and A. F. de O. Falcao, "Turbine-controlled wave energy absorption by oscillating water column devices," Ocean Eng. **17**, 481–497 (1990).
[5]W. Sheng, R. Alcorn, and S. Lewis, "On thermodynamics of primary energy conversion of OWC wave energy converters," J. Renewable Sustainable Energy **5**, 023105 (2013).

[6]A. Falcao, L. M. C. Gato, and E. P. A. S. Nunes, "A novel radial self-rectifying air turbine for use in wave energy converters," Renewable Energy **50**, 289–298 (2013).
[7]A. Falcao, J. C. C. Henriques, and J. J. Candido, "Dynamic and optimization of the OWC spar buoy wave energy converter," Renewable Energy **48**, 369–381 (2012).
[8]J. C. C. Henriques, A. Falcao, R. P. F. Gomes, and L. M. C. Gato, "Air turbine and primary converter matching in spar-buoy oscillating water column wave energy device," Proceedings of the 32nd International Conference on Ocean, Offshore and Arctic Engineering, June 9–14, 2013, Nantes, France.
[9]A. J. N. A. Sarmento and A. F. D. O. Falcao, "Wave generation by an oscillating surface pressure and its application in wave-energy extraction," J. Fluid Mech. **150**, 467–485 (1985).
[10]A. Thakker, T. S. Dhanasekaran, M. Takao, and T. Setoguchi, "Effects of compressibility on the performance of a wave-energy conversion device with an impulse turbine using a numerical simulation technique," Int. J. Rotating Mach. **9**, 443–450 (2003).
[11]W. Sheng, F. Thiebaut, M. Babuchon, J. Brooks, R. Alcorn, and A. Lewis, "Investigation to air compressibility of oscillating water column wave energy converters," Proceedings of the ASME 2013 32nd International Conference on Ocean, Offshore and Arctic Engineering, OMAE 2013, 9–14th June, 2013, Nantes, France.
[12]A. Falcao, L. M. C. Gato, and E. P. A. S. Nunes, "A new radial self-rectifying air turbine for use in OWC wave energy converters," Proceedings of the 9th European Wave and Tidal Energy Conference, 5–9 Sep. 2011, Southampton, UK.
[13]W. Sheng, R. Alcorn, and A. Lewis, "Numerical assessment on primary wave energy conversion of oscillating water columns (OMAE2014-23218)," Proceedings of the ASME 2014 33rd International Conference on Ocean, Offshore and Arctic Engineering, June 8–13, 2014, San Francisco, USA.
[14]W. Sheng, R. Alcorn, and A. W. Lewis, "Assessment of primary wave energy conversions of OWCs. I. Hydrodynamic analysis," J. Renewable Sustainable Energy **6**, 053113 (2014).
[15]S. A. Mavrakos and D. N. Konispoliatis, "Hydrodynamic analysis of a vertical axisymmetric oscillating water column device floating in finite depth waters," Proceedings of the ASME 31st International Conference on Ocean, Offshore and Arctic Engineering, July 1–6, 2012, Rio de Janeiro, Brazil.
[16]H. Martins-rivas and C.-C. Mei, "Wave power extraction from an oscillating water column along a straight coast," Ocean Eng. **36**, 426–433 (2009).
[17]W. Sheng, A. Lewis, and R. Alcorn, "On wave energy extraction of oscillating water column devices," Proceedings of the 4th International Conference on Ocean Energy, 17–19th October 2012, Dublin, Ireland.